PN-ABF-777

"Cooperative Research on Numerical Weather Prediction Related to Monsoons"

2. E-15

## FINAL REPORT

The activities under the project can be listed under three titles :

1. Training in Numerical Weather Prediction related to Monsoon :

Much progress has been made in establishing a centre in atmospheric science with emphasis on monsoon studies at IIT Kanpur. The funding from AID has enabled us to augment the scientific manpower, computer facilities, and data sets.

A workshop was conducted for six days in which seminars were given by scientists on Monsoon Climatology, Synoptic systems and observations. The lectures focussed on the numerical schemes and other basics essential for numerical modelling. There was an exchange of scientists between India and the USA for the purpose.

A one level primitive equation model and the Florida State University multi-level model were modified and run on computers in IIT Kanpur. Special data sets of the MONEX covering the ½ months of Monsoon period in 1979 and five year Indian station data sets were made available.

2. Numerical Weather Prediction Models :

(i) Objective analysis

One of the pre-requisites for NWP is the availability of data in a regular grid of the forecasting region from the irregular and sparse data network of observing stations in the region. Present methods of analysis may have to be modified for the Indian region which has large data voids in the oceanic areas. Preliminary work on the structure and correlation function of the moisture variable (q) indicates smaller scales and hence smaller scans in the objective analysis procedure. Also, the statistics and wind indicates the need for an elliptic instead of the present circular scan. Use of Chebyshev Polynomials and finite element techniques are also being studied. Mr P K Mishra from IITK completed the analysis of a number of fields and were found to be quite good. His results are being published at the present time.

Rec'd in SCI MAR 5 - 1990

(ii) One level primitive equation model

One of the IIT Kanpur students collaborated with Prof Krishnamurti for gaining experience in conducting forecast experiments. They carried out 980 forecasts with two simple high resolution regional models. These models are based on the principles of conservation of absolute vorticity (a stream function barotropic model) and of potential vorticity (the shallow water equations with botton topography). The results of the study show that the models show skill beyond persistence for a range of 4 days on integration, though the skill varied over different domains.

A number of forecasts without orography, utilising a single level P.E. model, with the 1979 MONEX data sets were made (upto 96 hours) at the IIT Kanpur Computer. The RMS statistics show that the model is of marginal utility for 24 hour forecasts but progressively improve against persistence with the length of the forecasts.

The chosen data sets were for the different phases; pre-onset, onset, active and depression. Future experiments run with orography and data initialization procedure are presently being carried out.

(iii) The FSU regional model

The project scientists familiarised themselves with the FSU multi-level grid point model on x,y,p system. A version of the FSU regional multi-level model is currently being implemented in India. The horizontal grid, its vertical analysis levels and vertical descretization is shown in fig. I and tables I and II respectively. This model is being tested as a possible operational model for the Indian Weather Service. It is now available for use at IITK. This model utilizes the so called sigma coordinate system where a maximum topographic height of 5600 m is being used over the Himalayas. It utilizes a one step semi-Lagrangian - semi-implicit time differencing scheme. Its physics includes radiatic processes, shallow and deep moist convection, dry convection adjustment, large scale condensation, surface fluxes following similarity theory and planetary boundary layer.

Initial balanced state is being achieved by using a new initialization scheme called 'Dynamic Normal Mode Initialization' proposed by M. Sugi. This scheme is dynamic initialization as it uses the forward-backward integration of the model. However, the fundamental idea of the scheme is also based on normal mode initialization and the results are equivalent to NMI. Further, this scheme includes physical processes.

The model program was transferred to DEC-system 10 which is the computer available at IITK. The program was made compatible with our system.

Table 1 **Analysis Levels**

| P | U | V | T | R.H | pressure |
|---|---|---|---|---|---|
| 100 | X | X | X | NOT REQUIRED | NOT REQUIRED |
| 200 | X | X | X | | |
| 300 | X | X | X | X | |
| 500 | X | X | X | X | |
| 700 | X | X | X | X | |
| 850 | X | X | X | X | |
| 1000 | X | X | X | X | |
| sea level | | | | | X |

Table II

## VERTICAL DESCRETIZATION

| $\sigma$ level | variables | level | variables |
|---|---|---|---|
| 0.1 | $P, \dot{\sigma}$ | | U,VT,R.H. |
| 0.2 | $P, \dot{\sigma}$ | | U,V,T,R°H. |
| 0.3 | $P, \dot{\sigma}$ | | U,V,T,R°H. |
| 0.4 | $P, \dot{\sigma}$ | | U,V,T,R°H. |
| 0.5 | $P, \dot{\sigma}$ | | U,V,T,R°H. |
| 0.6 | $P, \dot{\sigma}$ | | U,V,T,R°H. |
| 0.7 | $P, \dot{\sigma}$ | | U,V,T,R°H. |
| 0.8 | $P, \dot{\sigma}$ | | U,V,T.R°H. |
| 0.9 | $P, \dot{\sigma}$ | | U,V,T,R°H. |
| 1.0 | $P, \dot{\sigma}, P_s$ | | |

FIGURE 1

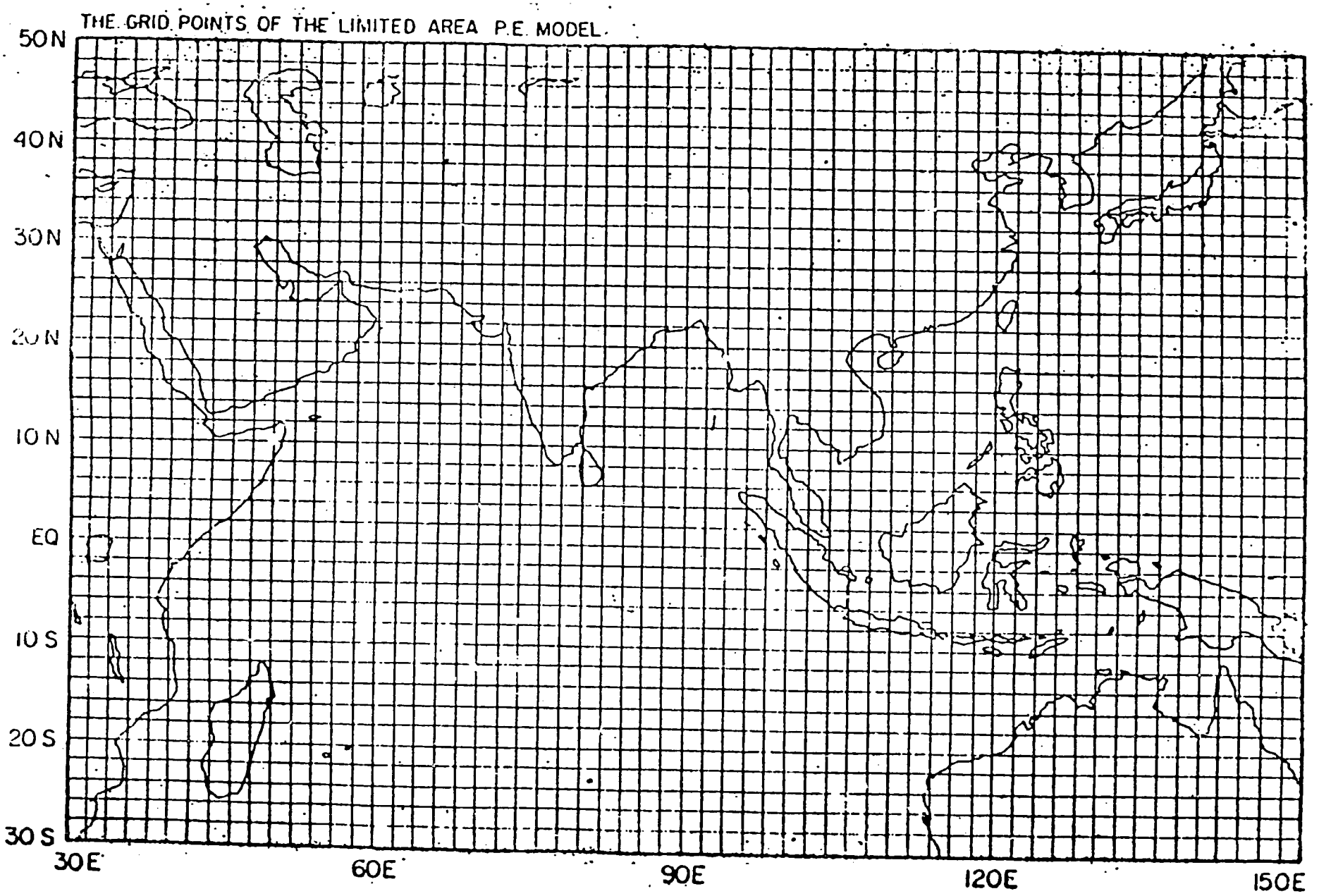
THE GRID POINTS OF THE LIMITED AREA P.E. MODEL
50N
40N
30N
20N
10N
EQ
10S
20S
30S
30E
60E
90E
120E
150E
J
1 — 41

It was debugged using a smaller horizontal area. Afterwards model domain in horizon- t[illegible]vas suitably cut down to 20°S to 45°N and 40°E to 112.5°E taking a 2.5° x 2.5° latitude longitude grid due to the computer memory limitations. Appropriate data was prepared. Presently, initialization is being run and the initialized fields are analysed. One of the studens of IITK is actively participating in the program. The model will be extensively tested. Our proposed experiments will include studies on the sensitivity of monsoon prediction to radiative processes.

(iv) Global spectral model

A version of this model available in the Florida State University was used by one of the IIT Kanpur scientists to make short range predictions on the onset phase of the Monsoon 1979 using the FGGE and MONEX data sets. The five day forecasts from 11 June 1979 were made on the CRAY in the Atmospheric Environment Service, Montreal. The results showed that the onset vortex formed on the third day as observed in the levels 500 mb to 850 mb and by day 5 developed into a depression. The energetics shoed that barotropic processes could be initially important especially at 850 mb. However the exchange of eddy potential energy to eddy kinetic energy was predominant after day 3 onwards. Vorticity budget computations showed the role of convection was direct as in tropical cyclones in providing a [illegible]ge vertical velocity and thereby the transport of vorticity by vertical advection. This is different from the Bay of Bengal depression with weak vertical velocities where the sub-grid scale processes by cumulus friction are known to provide the transport mechanism. Model forecasts showed rather a weaker wind maximum in the Somali region and a stronger one south of the vortex than the FGGE analysis. The forecast flow patterns in the equatorial and Somali regions were not as smooth as the FGGE analysis. Runs without the mountains still produced the vortex but they formed in the Central Arabian Sea and moved away from India. The results of these studies are accepted for publication in Mausam.

3. Observational and Theoretical Studies

(i) On the planetary scale changes during the onset 1979

FGGE III-b data sets for June 1979 were used to study the planetary scale changes in the upper and lower tropospheres during the onset phase. The largest contribution to the variance of the zonal component of the wind at the latitude of the monsoon jet (7.5°N) was from wave number one. This seems to be in response to the westward extension of the latent heating fields in the equatorial Indian Ocean fro[illegible]100 E to 50 E. At 300 mb significant changes preceded the onset in the middle

latitude (55°N) planetary scales. Here the wave numbers one and two weakened and their amplitude maximum shifted polewards and eastwards. The wave number three appeared to be largely due to orographic forcing.

(ii) Parameterization for cumulus convection

## Kuo's scheme for the estimation of moistening, heating and rainfall rates from Cumulus Convection

## INTRODUCTION :

### Kuo's Original Parameterization Procedure

Kuo utilized the following form of the moisture eqn.

$$\frac{\delta q}{\delta t} = a \frac{q_s - q}{\Delta \tau} \qquad (1)$$

is a cloud time scale parameter and a denotes the fraction area of the grid scale that would be covered by newly formed convective clouds. The parameter a is defined by the relation

$$a = \frac{-\frac{1}{g} \int_{P_T}^{P_B} \left( \nabla . q\vec{V} + \frac{\delta}{\delta p} q\,\omega \right) dp}{\frac{1}{g} \int_{P_T}^{P_B} \frac{C_p(T_s - T)}{L\,\Delta\tau} + \frac{q_s - q}{\Delta\tau}\, dp} \qquad (2)$$

Symbol Q may be used to represent the denominator of the above eq$^n$. Here $P_B$ denotes the cloud base and $P_T$ cloud top. These are the lifting condensation level and the level where the moist adiabat intersects the environmental sounding. The parameter a is also written as

$$a = \frac{\text{Measure of the available moisture supply}}{\text{Amount of moisture supply needed tocover the entire grid scale by a model cloud.}}$$

The convective rainfall rate is given by the relation,

$$P_T = \frac{1}{g} \int_{P_T}^{P_B} \frac{a\, C_p(T_s - T)}{L\,\Delta\tau}\, dp \qquad (3)$$

We know that part of moisture convergence, I, is used for raising the level

of moisture and part of it goes into condensation heating. This partitioning may be expressed by the relation

$$I = I_q + I_\theta$$

This scheme is unsatisfactory for large scale applications. This was discussed by Krishnamurti et al. (1980) and several others.

The available moisture supply, I, is disproportionately partitioned among the moistening and heating; more of the supply goes into moistening, thus causing an early saturation prior to the establishment of the neutral moist adiabatic sounding on the large scale. The heating rates and the rainfall totals are usually underestimated in studies when the grid size is of the order of a few 100 km.

As an extension we next use the following form of the thermal and moisture equations :

$$\frac{D\theta}{Dt} = -\frac{\omega\delta\theta}{\delta p} + a_\theta \left[ \frac{\omega\delta\theta}{\delta p} + \frac{\theta}{T} \frac{(T_s - T)}{\Delta\tau} \right] \qquad (4)$$

$$\frac{Dq}{Dt} = a_q \cdot \frac{q_s - q}{\Delta\tau} \qquad (5)$$

We have a cloud layer between $P = P_T$ and $P = P_B$. In this region no explicit evaporation is used. We shall define here the available moisture supply, I, by the relation

$$I = -\frac{1}{g} \int_{P_T}^{P_B} \omega \frac{\delta q}{qp} \, dp \qquad (6)$$

Furthermore, we define two functions,

$$Q_\theta = \frac{1}{g} \int_{P_T}^{P_B} \frac{C_p}{L} \left[ \frac{T_s - T}{\Delta\tau} + \frac{T}{\theta} \omega \frac{\delta\theta}{\delta p} \right] d\theta \qquad (7)$$

$$Q_q = \frac{1}{g} \int_{P_T}^{P_B} \frac{(q_s - q)}{\Delta\tau} \, dp \qquad (8)$$

These two functions $Q_\theta$ and $Q_q$ are known and $Q = Q_\theta + Q_q$ is a measure of total moisture supply needed to cover a volume over a unit horizontal area with clouds.

We next divide I into two parts

$$I = I_\theta + I_q \qquad (9)$$

Where $I_\theta$ is a part of the moisture supply which goes into enhancing the tempe-

rature field, and $I_q$ is a part that modifies the moisture field. Let us introduce two unknown $a_\theta$ and $a_q$ by the relations,

$$a_\theta = I_\theta / Q_\theta \tag{10}$$

and

$$a_q = I_q / Q_q \tag{11}$$

Thus we obtain,

$$a_q Q_q + a_\theta Q_\theta = I = I_q + I_\theta \tag{12}$$

This equation has two unknown $a_q$ and $a_\theta$.

Let

$$a_q Q_q = b I \tag{13}$$

then

$$a_\theta Q_\theta = (1-b) I \tag{14}$$

The parameter b (a moistening parameter) is the only unknown at this stage.

A major improvement in the estimates of heating and rainfall rates came by assuming that that all of the mositure supply rains out, i.e. b = 0.

An alternative was recently proposed by Krishnamurti et.al (1983) where a mesoscale convergence parameter, $\eta$, was introduced as an additional contributor to the large scale moisture supply.

The mesoscale convergence parameter $\eta$, and moistening parameter, b were expressed as function of large scale variables using statistical multiple regression methods as a function of the large scale observations from the GARP Atlantic Tropical Experiment. A statistical relation between vertically integrated vertical velocity and relative vorticity is obtained at 700 mb.

$$\eta = a_1 \xi + b_1 \bar{\omega} + c_1$$

$$b = a_2 \xi + b_2 \bar{\omega} + c_2$$

where

$$a_1 = 0.265 \times 10^5 \quad ; \quad a_2 = 0.158 \times 10^5$$

$$b_1 = 0.411 \times 10^3 \quad ; \quad b_2 = 0.304 \times 10^3$$

$$c_1 = 0.346 \quad ; \quad c_2 = 0.476$$

In a prediction model the effects of cumulus scale heating and moistening are expressed by

$$\frac{\delta\theta}{\delta t} + \vec{V}.\nabla\theta + \omega\frac{\delta\theta}{\delta p} = a_\theta\left(\frac{\theta_s - \theta}{\Delta\tau} + \omega\frac{\delta\theta}{\delta p}\right) \quad (17)$$

$$\frac{\delta q}{\delta t} + \vec{V}.\nabla q = a_q\left(\frac{q_s - q}{\Delta\tau}\right) \quad (18)$$

The terms on the right hand side denote the cumulus effects.

The coefficients $a_\theta$ and $a_q$ will next be expressed as functions of the parameter and b. The total moisture supply is given by $I(1+\eta)$. This is divided into two parts namely : $I(1+\eta)(1-b)$ goes into heating and $I(1+\eta)$ goes into moistening.

Thus $a_\theta = I(1+\eta)(1-b)/Q_\theta$ (19)

and $a_q = I(1+\eta)b/Q_q$ (20)

Thus application of this more general method requires :

i) a determination of b and $\eta$ as a function of large scale variable.

ii) evaluation of $a_\theta$ and $a_q$ as a function of b and $\eta$.

This code can be easily transformed to yield the heating and moistening by the classical Kuo scheme. For this purpose one must redefine b and $\eta$. i.e.

Let $b \equiv \frac{Q_q}{Q_o}$ and $\eta =$

Rainfall rate

$$P_T = \frac{1}{Lg}\int_{P_T}^{P_B} a\left[\omega\frac{\delta\theta}{\delta p} + \left(\frac{P_o}{p}\right)^{R/C_p}\frac{C_p(T_s - T)}{\Delta\tau}\right]dp \quad (21)$$

Thus we obtain

$$\frac{I_q}{Q_q} = \frac{I_\theta}{Q_\theta} = \frac{I_L}{Q} = \frac{I}{Q} \quad (22)$$

Furthermore, if following Kuo (1965), we define

$$a = I/Q$$

then we note that $a_\theta = a_q = a$.

The intermediate scheme based on Kuo (1974) can also be coded by putting

$$\eta = 0. \text{ and } b = 0.$$

Computational studies :

The Kuo's scheme developed by Krishnamurti et al (1983) is planned to be tested in the monsoon region first in a semi-prognostic approach and later with a regional prediction model. The area chosen for the one time-step semi-prognostic method is the triangular region formed by Minicoy, Trivandrum and Mangalore. Preliminary studies indicate that the constants suggested in Krishnamurti et al (1983) may need to be modified for obtained realistic rainfall rates. Data for 1977 and 1979 are used and further studies are in progress.*

(iii) Atmospheric waves

Analysis of waves in mid-latitudes is at a more advanced stage than in tropical equatorial regions. We find that there is need for clarifying the dynamics of even the free wave on a realistic basic state. Our analysis has shown that to study the Rossby Gravity waves in tropical-equatorial region one cannot neglect the vertical component of the Coriolis force. However, incorporating the vertical component leads to the mathematical problem of separability. We have succeeded in overcoming this problem. Now there is an unambiguous definition of Rossby Gravity Waves as distinct from Internal Gravity Waves all the way to the equator. Our treatment of both kind of waves has another important feature. The boundary condition is more appropriate for the study of tropospheric processes. We require vanishing vertical component of the velocity at the ground and a radiation condition at the tropopause. Next stage of the effort on this route took us to the study of heating and atmospheric wave response to it. The radiative boundary condition now is taken very seriously. We think that the traditional approach of analyzing the response in terms of normal modes needs to be changed. Normal mode analysis requires a lid at the tropopause which infact is not there. The lid may be an acceptable idealization while discussing flows but for waves it shuts up a very important mode of transport of energy upward. Thus, in our study we do not use normal modes, we use waves with radiative boundary condition at the tropopause and vanishing vertical velocity at the ground. We have studied gravity waves response to local heating. The expression for energy flow in closed form has been obtained. The associated integrals have been computed for a series of points and a series of instants bringing out the pattern of energy flow. A similar work on Rossby Gravity Wave response to a pattern of global heating has also been computed. Rossby gravity wave response to heating is more involved because the waves have a characteristic meridional as well as vertical profile whereas gravity waves have a characteristic

profile only vertically. The expression for flow of energy has been obtained and suitably plotted. This work is also being submitted for publication.

The mathematical control over the otherwise vast equations that has been acquired has given us a good head start in studying some of the problems in mean-flow-wave interactions. A better understanding of free waves has also been important. This work has just begun.

We are now able to propose an initialization scheme. It is akin to the non-linear normal mode initialization without the normal modes. Our gravity waves are not normal modes or their superpositions. They satisfy radiation boundary conditions. Further, unlike the normal modes that are characteristic of the whole atmosphere (with its lid) as expressed through the specific numerical model, our gravity waves are characterized by heat sources. This has the very important consequence that initialization of these gravity waves will do no violence to the heating pattern and associated meanflow. It may be recalled that initialization in the equatorial regions so far have faced two major stumbling blocks. One is that it kills convection and Hadley cells which are just not dispensable. The other is a proper understanding of gravity waves and Rossby gravity waves and their distinction near the equator. We think that we have atleast the beginnings of answers to both these questions. Hence we are optimistic of the proposed initialization scheme.

(iv) Rainfall Distribution on the Leeside of Western Ghats

During the South-west monsoon heavy rainfall is concentrated on the windward slopes of Western Ghats mountains of India and there exists a rain shadow on the leeside towards the east. This general distribution of rainfall in relation to orography would appear to be firmly consistent with the kinematic properties of mean air motion in which vertical velocity is upward on the windward side and downward on the leeside. A study of the amount and distribution of the rainfall on the mesoscale taking into account the dynamics of air motion in and around the mountain was made by Queney (1970), Sarker (1966,1967), Smith (1979,1981) Grossman et al. (1984) etc. On the basis of the theoretical result Sarker concludes that while the peak in the rainfall distribution is entirely due to orography, the same cannot be said about the rainfall on the leeside. Grossman et al. believe that partial deceleration of the monsoon flow by upstream blocking effects of the mountains initiates and maintains a vertical and horizontal motion field that could support the observed convection. It is well known that summer monsoon current is not a steady air current being marked by frequent passage of convergence or divergence

patterns mostly associated with the perturbations or depressions. Under the influence of these synoptic scale convergence or divergence patterns, the distribution of vertical velocity due to orography may be considerably modified with consequent modification in the distribution of rainfall.

The present report gives the results of a study aimed at demonstrating the effect of synoptic scale disturbance in the form of a monsoon depression upon the amount and distribution of rainfall in the Western Ghats region. In this study, attempt is made to quantitatively relate computed vertical velocity at orographic surface and above in the lower troposphere with observed rainfall. Analyzing the MONEX 79 data a second maximum around 40 km from the peak of Western Ghats in the leeside could not be reproduced in this model as used by Sarker. Rainfall on the leeside may occur from other contributing factors such as instability due to vertical wind shear of the mean horizontal zonal velocity field. Or may be since the monsoon air is conditionally unstable in the forced ascent upto the level of lifting condensation results in rainfall. Hence the rainfall is generally assumed to be proportional to the upward vertical velocity. Therefore we are trying to introduce a time dependent perturbation which allows energy and momentum exchange between the mean field variables and perturbations. Calculation of vertical velocity with appropriate boundary conditions is expected to give a more realistic value. Rainfall distribution on the leeside is also expected to be more closed to reality in this model.**

(v) Lorenz Attractors and Initialization

Initialization problem of NWP can be viewed as finding attractions of the dynamical system (Lorenz, 1980). We have seen in another study (Ray, 1985) that the system dynamical equations of shallow water model, have attractors for some parametric setting. We found that Lorenz parameter r depends on forcing, diffusivity parameter and Rossby number of the flow. We came to the conclusion that primitive equation model and quasigeostrophic model equations behave differently. Also, we have seen, making all other parameters same, only variation in Rossby number (which is the parameter for distinguishing between middle latitude and tropical latitude) results in quite interesting behaviour after some days of integration. In one case (middle latitude) primitive equation model behaves like quasi-geostrophic model after some days of integration; in other case, stream function and height variable remain separated. The difference in behaviour of primitive equation model for tropics and middle latitude remains a quite interesting study.

In the present study we try to analyse contributions of linear and non-linear terms to the time tendencies of the variables. We find that linear and non-linear analysis of the dynamical equations for middle latitude and tropics are

different. The balance relation depends on Rossby number and consequently slow manifold (Leith, 1980) is not unique.

## REFERENCES*


1. Kuo, H.L., (1965) : On formation and intensification of tropical cyclones through latent heat release by Cumulus Convection. J.Atmos. 22, 40-63.
2. Kuo, H.L., (1974) : Further studies of the parameterization of the influence of cumulus on large scale flow. J.Atmos. 31, 1232-1240.
3. Krishnamurti, T.N., Y. Ramanathan, H. Pan, R. Pasch and J. Molinari,(1980): Cumulus paraterization and rainfall rates I. Mon.Wea.Rev., 108, 465-472.
4. Krishnamurti, T.N., S. Low-Nam and R. Pasch, (1983): Cumulus parameterization and rainfall rates II. Mon.Wea.Rev., 111, 815-828.

## REFERENCES**


1. Grossman, Robert L and Dale R Durran (194) : Interaction of low level flow with the Western Ghats mountains and offshore convection in the summer monsoon. Mon.Wea.Rev. (112) 652-672.
2. Sarker, R.P. (1966) : A dynamical model of orographic rainfall. Mon.Wea.Re. (94) 555-572.
3. Sarker, R.P. (1967) : Some modification in a dynamical model of orographic rainfall. Mon.Wea.Rev. (95) 673-684.
4. Smith, R.B. (1979) : The influence of mountain on the Atmosphere. Advances in Geophysics. Vol.21. Academic Press 186-288.
5. Smith, R.B. (1981) : A differential advective model of orographic rain. Mon. Wea.Rev. (110) 306-309.
6. Queney, P. (1970) : Transfer and dissipation of energy by Mountain waves. Dynamics Meteorology edited by P. Morel.

# NUMERICAL WEATHER PREDICTION EXPERIMENTS OVER THE MONSOON REGION

KHALIF ATMA[1]

ARUN KUMAR[2],

T. N. KRISHNAMURTI[1]

[1]Department of Meteorology
Florida State University
Tallahassee, Florida 32306

[2]Indian Institute of
Technology, Kanpur,
Kanpur 208016, INDIA

Supported by
A.I.D.

FSU Report No. 84-6
August 1984

14

CONTENTS

Abbreviations

List of Symbols

Abstract

1. Introduction

2. Domain integration

3. The Models

3.1 Nondivergent Barotropic model

3.1.1 Basic Equation

3.1.2 Domain invariant

3.2 Divergent Barotropic model

3.2.1 Basic Equation

3.2.2 Domain invariant

3.2.3 Bottom topography

3.2.4 Dynamic Initialization

4. Time Difference scheme

5. Boundary condition and Smoothing

6. Data source and Computation of Streamfunction

7. Verification system

8. Concluding remark

9. Reference

Abreviation :

| | | |
|---|---|---|
| ECMWF | : | European Centre for Medium range Weather Forecast. |
| FGGE | : | First GARP Global Experiment. |
| GARP | : | Global Atmospheric Research Programe. |
| GATE | : | GARP Atlantic Tropical Experiment. |
| Monex | : | Monsoon Experiment. |
| NOAA | : | National Oceanic and Atmospheric Administration. |
| NWP | : | Numerical Weather Prediction. |
| 1LPE | : | One Level Primitive Equation. |
| RMSE | : | Root Mean Square Error. |
| WMO | : | World Meteorological Organization. |
| W W W | : | World Weather Watch. |

List of Symbols.

$c$ : Phase of speed.

$f$ : Coriolis parameter.

$g$ : Earth's gravity.

$h$ : Terrain height.

$u$ : zonal wind component.

$v$ : Meridional wind component.

$z$ : free surface height.

$K$ : Kinetic energy.

$J$ : Jacobian operator.

$\nabla^2$ : Laplacian operator.

$\frac{d}{dt}$ : Lagrangian operator.

$\beta$ : Beta parameter.

$\partial x$ : Zonal derivative.

$\partial y$ : Meridional derivative.

$\zeta$ : Relative Vorticity.

$\zeta_a$ : Absolute vorticity.

$\zeta_p$ : Potential vorticity.

$\varphi$ : Latitude

$\psi$ : Streamfunction.

$E_T$ : Energy total

$V_n$ : Normal wind.

$(\langle K_z \cdot K_E \rangle)$ : Barotropic energy conversion.

$(\bar{\ })$ : Domain average.

$i$ : number of zonal grid points.

$j$ : Number of meridional grid points.

$F$ : Forecast value.

: Parameter value.

$B$ : Boundary.

$A_V$ : Verified value.

$A_o$ : Initial value.

$C$ : Climatological value.

$g_i$ : Weighting factor.

Abstract

The predictive capability of the conventional single level models is examined here. The area concerned during integration is over Arabian sea, Indian continent and its ocean and the south east Asia. A review of basic equations form the frame work of the models is presented. Finite difference scheme, boundary - condition and smoothing procedure are also briefly discussed. The 96 hours predictive capability are assessed by calculating RMSE and Absolute Correlation of the motion field over small verification area inner the domain integration. This experiment is based on 61 set of data obtained from FGGE/monex during northern summer season as the initial analysis state. Results of 96 hours forecast of few days experiment as samples are plotted and discussed.

## 1. Introduction.

The region of Southeast Asia, Indian continent and its ocean have characteristicaly a strong monsoon flow. The predictive capability of the conventional single level model over Southeast Asia during winter monsoon has been conducted by Yap, K.S. (1983) His domain integration was expanded to the west pacific region. He noted that the single level model over southeast Asia during winter shows somewhat poor performance when compared to persistence It probably, during winter, the rainy season over Southeast Asia dominated the divergent/convergent flow.

In this study we atempted to investigate the predictive capability of the single level models over these monsoon region during northern summer season. Those single level models are the nondivergent barotropic model and the divergent barotropic model. The later is also called one level primitive equation (1LPE).

In the formulation of those models, physical processes are essentially absent. Those models consider some dynamical property conservations such as absolute vorticity for the nondivergent barotropic model and potential vorticity for the One level primitive equation model. The level of isobaric surface chosen in this study is 700 mb. This is essentially following Krishnamurti and Adejokun (1983) who showed that this level is of considerable a good approximation of the nondivergent level over tropical area and it has the largest amplitude of tropical wave.

The data used for the initial state come from the rich documentation data set of FGGE/Monex. The data source and its analysis is briefly discussed in one section. In the tropical region, persistence is of considerable a good performance. In this study, therefore, the forecast skills are compared to persistence. The forecast skills are assessed by measuring RMSE of field motion, Absolute Correlation and Anomaly Corretion. The verification systim is following Neimen R. (1983). The good performance of those single level is expected to be useful things for further improvement of numerical analysis over this tropical monsoon region.

## 2. Domain integration.

We chosed the domain integration over the area of 30°S-40°N latitude and 30°E-150°E longitude, with 1.875° grid mesh. This grid size was chosen as it is original data from FGGE/monex. The domain was also made cyclic in the east-west boundary during integration.

## 3. The Models.

### 3.1 Nondivergent barotropic model.

#### 3.1.1 Basic equation.

The conservation of absolute vorticity has been used to form the basic dynamic equation. The familiar relation of this principle can be written in term of streamfunction, $\psi$, as :

$$\frac{\partial}{\partial t}\nabla^2\psi = -J(\psi, \nabla^2\psi) - \beta\frac{\partial\psi}{\partial y} \qquad \text{..... (1)}$$

The equation (1) above is a basic frame work for nondivergent barotropic model used in this study.

#### 3.1.2 Domain invariant.

This model should contruct not only mean absolute vorticity of the domain ($\overline{\zeta_a}$) to be conserved, but also mean absolute vorticity square ($\overline{\zeta_a^2}$) and barotropic kinetic energy ($K_E$). Another - property which should be invariant in the domain is the barotropic energy exchange ($\langle K_z \cdot K_e \rangle$).

In order to make those properties conserve, the advective term : $J(\psi, \zeta)$ is accomplished by using Arakawa jacobian following Arakawa (1966). To represent $\nabla^2$, we used standard of second order of Laplacian.

3.2 Divergent barotropic model.

The second model studied here is the model which allows the presence of divergence. This model is also called :

1. One level primitive equation
2. Shallow water equation
3. Laplace's tidal equation

3.2.1 Basic equation.

The basic equation forms the frame work of this model is described by the horizontal equation of motion and mass continuity equation. There are three equation with three unknowns, u, v, and z.

$$\frac{\partial u}{\partial t} + u\frac{\partial u}{\partial x} + v\frac{\partial u}{\partial y} - fv = -g\frac{\partial}{\partial x}(z+h) \qquad \text{..... (2)}$$

$$\frac{\partial v}{\partial t} + u\frac{\partial v}{\partial x} + v\frac{\partial v}{\partial y} + fu = -g\frac{\partial}{\partial y}(z+h) \qquad \text{..... (3)}$$

$$\frac{dz}{dt} = -z\,\nabla\cdot\vec{V} \qquad \text{..... (4)}$$

3.2.2 Domain invariant.

The domain invariant of this model are the potential vorticity $\zeta_p = \frac{\zeta + f}{z}$ and its power $(\overline{\zeta_p^n})$, a total energy $E_t = z(K + gz/2 + gh)$ and mean height of the free surface $\bar{z}$.

3.2.3 Bottom topography.

In the shallow water equation, free surface height can be expressed linierly as mean free surface height and its perturbation, that is :

$$z = \bar{z} + z' \qquad \text{..... (5)}$$

If we subtitude eq.(2) and eq.(3) we can show that there is a relation between mean surface height $\bar{z}$ and the phase speed of wave (c)

$$c = u \pm \sqrt{gz} \qquad \ldots\ldots\ldots\ldots\ldots\ldots\ldots (6)$$

This shows that z plays an important role in the shallow water equation model, and hence z. Ploshay (1977) has shown that the value of 2000 meter as mean free surface height gives a realistic phase speed and amplitude of the African wave. Krishnamurti and Adejokun (1980) in the study to 700 mb GATE area forecast - also gave a similar conclution.

From those experiment explained above we fixed the value of 2000 meter as mean free surface height used in this study. We also used the bottom topography as it was mentioned by Krishnamurti (1979) that using the bottom topography improved forecast over GATE area. The bottom topography utilized in this study has been modified by the relation :

$$h_{modified} = h_{original} \times \frac{1500}{r_{max}} \qquad \ldots\ldots\ldots\ldots (7)$$

The bottom topography field obtained from Gates and Nelson (1975) and interpolated into 1.875° grid mesh.

### 3.2.4 Dynamic initialization.

The z field that used in the divergent barotropic model is obtained from initial analysis of streamlines and isotachs using nonlinear balance equation. This causes the horizontal - motion and pressure field inequilibrium. In order to adjust the motion and the pressure field in an equilibrium, the forward-back ward was integrated iteratively utilizing small time steps. The value of 600 second was utilized as time step for dynamic initialization in this study.

4. Time difference scheme.

The semi lagrangian advection following Krishnamurti (1969) and Matsuno (1970) has been used here during the integration of Eq.(2),(3) and (4). Euler forward-backward following Matsuno (1966) which involves predictor corrector was utilized to accomplish time difference scheme. Time step of 2700 second was used during integration of both nondivergent and divergent barotropic model. The time step was chosen based on Courant Federich Levy criterion, that is :

$$\Delta t = \frac{\Delta x}{(c + u_{max})} \qquad \ldots\ldots\ldots\ldots\ldots\ldots \quad (8)$$

5. Boundary condition and Smoothing.

The boundary condition values in both nondivergent and divergent barotropic models essentially followed what was done by Krishnamurti (1969). The u and v component at the south-north boundary were set to be constant while being allowed to vary - zonally. In the east-west direction the boundary condition was made cyclic by extending about 1000 km or six grid points beyond the domain analysis. These artificial points were made to remove east-west boundary or to make smooth cyclic continuity of map. Western boundary were set to be the same as eastern boundary - value, and the other artificial points were calculated by using linier interpolation.

At the south-north boundary, the discontinuity at adjecent point tends to be occured caused by the open boundary. In order to reduce this discontinuity the smoothing procedure proposed by Shuman (1957) has been utilized in this study.

The smoothing formula is :

$$F_{i,j} = \alpha(F_{i,j}) + \tfrac{1}{2}(1-\alpha)(F_{i,j+1} + F_{i,j-1}) \quad \ldots\ldots\ldots \quad (9)$$

The value of $\alpha = .95$ was used here during the smoothing procedure.

6. Data source and Computation of streamfunction.

The data used in this study come from the FGGE IIa and Monex IIa data set, which were colected by special observation such as cloud wind and cloud imaginary from geostationary satellite drop wind sounde from research aircraft, constant level ballons, ships and enhenced network of WWW station. The quality of the data was assessed in terms of agreement with other data types and its space-time continuity. The dropwind sounde data during summer monex was of high quality.

Initial analysis of these data were done following Krishnamurti and Tripoli (1975) using the method proposed by Bergthorson and Dòòs (1955) and Cressman (1959). The method was using 4 passes of the successive correction, which in each analysis reduced the radius of influence. The first guess field used for initial was FGGE IIIa data set.

The initial streamfunction used in both divergent and non-divergent barotropic models has been difined by the initial horizontal wind following Krishnamurti (1969). The method of subsequential relaxation was used to calculate $\psi$ from the Poison's equation $\nabla^2\psi$. This relaxation method was also utilized during the integration of 96 hours streamfunction, because this method is much faster than the other usual relaxation.

The initial streamfunction at the boundary was calculated from initial horizontal wind at the boundary regarding the conservation of mass over the computational domain. Small correction was made to the normal wind at the boundary such that the line integral over the domain is zero. The modified normal wind values then can be expressed as :

$$V_n^{*} = V_n + \varepsilon |V_n| \qquad \ldots\ldots\ldots\ldots\ldots\ldots\ldots\ldots(10)$$

$$\varepsilon = \frac{-\int_B V_n \, dl}{\int_B |V_n| \, dl}$$

The streamfunction at the boundary can be calculated from the normal wind using the relation :

$$u = -\frac{\partial \psi}{\partial y}$$

and

$$v = \frac{\partial \psi}{\partial x}$$

7. <u>Verification system</u>.

Verification score studied here is essentially following as suggested by WMO/CAS working group weather prediction research (1978) for NWP product. These verification score recomended are :

1. RMSE for forecast and persistence
2. Absolute correlation for forecast and persistence
3. Anomaly correlation for forecast and persistence

We get the expressions for objective scores :

1. RMSE of forecast : $\sqrt{\dfrac{\Sigma(F-A_v)^2 g_i}{\Sigma g_i}}$

2. RMSE of persistence : $\sqrt{\dfrac{\Sigma(A_o-A_v)^2 g_i}{\Sigma g_i}}$

3. Absolute Correlation of forecast : $\dfrac{\Sigma[(F-F)(A_v-A_v)]\, g_i}{\sqrt{\Sigma(F-F)^2 g_i \Sigma(A_v-A_v)^2 g_i}}$

4. Absolute correlation of persistence : $\dfrac{\Sigma[(A_o-A_v)(A_v-A_v)]\, g_i}{\sqrt{\Sigma(A_o-A_v)^2 g_i \Sigma(A_v-A_v)^2 g_i}}$

5. Anomaly correlation of forecast :

$$\frac{\Sigma\left[\{(F-C)-(F-C)\}\ \{(A_v-C)-(A_v-C)\}\right] g_i}{\sqrt{\Sigma[(F-C)-(F-C)]^2 g_i \Sigma[(A_v-C)-(A_v-C)]^2 g_i}}$$

6. Anomaly correlation of persistence :

$$\frac{\left[\{(A_o-C)-(A_o-C)\}\ \{(A_o-C)-(A_o-C)\}\right] g_i}{\sqrt{\Sigma[(A_o-C)-(A_o-C)]^2\ g_i \Sigma[(A_o-C)-(A_o-C)]^2\ g_i}}$$

Cosines of latitude has been used as weight factor ($g_i$) in this objectives score calculations.

RMSE. As it was mentioned in previous study, Adejokun (1983), the RMSE is good way of estimating the performance of both baro tropic and 1LPE models. The smaller the RMSE, the better perform ance of the verified parameter.

Absolute Correlation. This skill score has been used to measure the correlation between the verified parameter and the referent parameter value. The value of greater than 0.5 for Absolute corr elation is considerably accepted as a good skill (Hollingwort.et al 1980).

Anomaly Correlation. This skill score is similar to Absolute Correlation, but it uses the climatological value as the referent parameter. The climatological value used in this study was obtained by averaging the parameter value at every grid point over 61 experiments. The Anomaly correlation will show the correlation between the forecast or the observed and climatological value.

Those verification score are calculated in two cases. Cas 1. is verification score for forecast. The verification score in this case is calculated between the forecast and its observed value (actual value). Case 2. is the verification for persistence. This calculates the statistic error between initial state value utilized to obtain forecast and the observed value related to its forecast.

Those verification score are calculated for each component of u and v. Hence, the verification of vector wind can be obtained from :

$$\text{RMSE (vector)} = \sqrt{\text{RMSE}^2(u) + \text{RMSE}^2(v)}$$

$$\text{Abs. Correlation (vector)} = \sqrt{\tfrac{1}{2}(\text{Abs.Corr}^2(u) + \text{Abs.Corr}^2(v))}$$

$$\text{Anomaly Correlation (vector)} = \sqrt{\tfrac{1}{2}(\text{An. Corr}^2(u) + \text{An. Corr}^2(v))}$$

The computation of those objectives was done over a limited area inner domain bounded by longitudes 50°E to 130°E and latitudes 15°S to 25°N. This was done in order to reduce the error caused by the open boundary and at adjacent points closed to boundary.

8. Concluding Remark.

Flow pattern. The flow field obtained from the experiment can be seen on figure 1. to 7. (a,b and c). Those are some - examples of the flow field chosen to be presented here. The area covered in those examples is smaller than the domain integration area. They show the forecast of both models from 24 hours to 96 hours and their actual field of June 2, June 3, June 4 and June 5.

Those figures show a good agreement between observed and forecast of the significant pattern such as trough and ridge - over this tropical area especially for the first 24 hours of forecast. Because of the involvement of terrain heigh, ILPE model shows better performance over mountains of Asia than that of barotropic model.

From those examples, therefore, the 1LPE model's forecast appears comparably more realistic than that of the barotropic - model. From those figures , we conclude that for barotropic - model the forecast skill is considerably reasonable during the first 24 hours, while for the 1LPE model up to 48 hours.

Statistic errors. The statistic errors of RMSE, Abs. Correlation and Anomaly Correlation for forecast and persistence of June 1, June 2, June 3 and June 4 are presented in Tables 1,2,3 and 4 respectively. On table 5, the statistic errors are averaged over 57 of data experiment and also compared to the previous studies.

From those examples of statistic error we found that only few of RMSE of barotropic model show better performance. In general, the performance of 1LPE model is better than that of barotropic model although the performance of forecast for both models is somewhat poor compared to the persistence. Table 5. shows - that those RMSE of 96 hours forecast look reasonable compared to previous studies. Abs. Correlation and Anomaly Correlation show a good correlation for 24 hours forecast for both models.

Domain invariant. Table 6a and 6b. show the domain invariant of barotropic and 1LPE model. Those show a good invariant. For 1LPE model the domain invariant of all properties does not depart more than 5 %, while for barotropic model the kinetic energy shows departure up to 21 %, but for the others show a good - invariant. This unconserved of kinetic energy may be caused by the open boundary system.

It should be noted that in this experiment the forecast skill of both single models give a good performance only for the first ten days (June 1, up to June 10). If we look at summer monex atlas part II we find that either westerly monsoon over India or easterly monsoon over Indonesia has not showed strong activity during the first ten days of June 1979. After that - period both monsoon over India and over Indonesia showed their activity for troughout the summer season, and accompanied by the existence of tropical easterly jet stream at high level troposphere. The tropical easterly jet stream occurence is followed by the direct Hadley cell. This Hadley strong overturning essentially controls day to day flow field over this tropical region. The occurence of tropical easterly jet stream accompanied by strong Hadley overturning is a persistent feature over extreme Souteast Asia during the North hemisphere summer season.

For further improvement of result, we would suggest that the physical processes should be added to the model so that such a realistic phenomenon can be carried out.

Acknowledgement.

This work was supported by the Agency for International Development and the International Office of the National Science Foundation under grants DPE-552G-SS3009-00 and NSF/SFC Grant INT 82-19026.

Table 1. RMSE, Absolute Correlation and Anomaly Correlation for Borotropio model, 1LPE model and Persistence. Initial state June 1, 1979.

Table 2. RMSE, Absolute Correlation and Anomaly Correlation for Barotropic model, 1LPE model and Persistence. Initial state June 2, 1979.

1.

JUNE 1,1979

| | 1LPE | BARO | PERSIST |
|---|---|---|---|
| RMSE (M/SEC) | | | |
| (1) VECTOR WIND | | | |
| 24 HRS | 3.177 | 4.100 | 3.691 |
| 48 HRS | 4.052 | 6.385 | 5.268 |
| 72 HRS | 5.075 | 8.292 | 6.093 |
| 96 HRS | 5.623 | 7.919 | 6.351 |
| (2) ZONAL WIND | | | |
| 24 HRS | 2.355 | 2.955 | 3.031 |
| 48 HRS | 3.242 | 5.416 | 4.335 |
| 72 HRS | 4.259 | 7.738 | 5.053 |
| 96 HRS | 4.582 | 7.067 | 4.973 |
| (3) MERIDIONAL WIND | | | |
| 24 HRS | 2.133 | 2.842 | 2.107 |
| 48 HRS | 2.431 | 3.381 | 2.993 |
| 72 HRS | 2.760 | 2.980 | 3.405 |
| 96 HRS | 3.260 | 3.573 | 3.950 |
| ABS.CORRELATION | | | |
| 24 HRS | 0.743 | 0.736 | 0.730 |
| 48 HRS | 0.593 | 0.460 | 0.424 |
| 72 HRS | 0.401 | 0.275 | 0.292 |
| 96 HRS | 0.296 | 0.206 | 0.307 |
| AND.CORRELATION | | | |
| 24 HRS | 0.856 | 0.789 | 0.799 |
| 48 HRS | 0.758 | 0.425 | 0.600 |
| 72 HRS | 0.585 | 0.071 | 0.480 |
| 96 HRS | 0.476 | 0.264 | 0.459 |

2.

JUNE 2,1979

| | 1LPE | BARO | PERSIST |
|---|---|---|---|
| RMSE (M/SEC) | | | |
| (1) VECTOR WIND | | | |
| 24 HRS | 3.032 | 3.914 | 3.485 |
| 48 HRS | 4.321 | 7.399 | 4.795 |
| 72 HRS | 5.229 | 8.705 | 5.778 |
| 96 HRS | 5.934 | 8.973 | 5.658 |
| (2) ZONAL WIND | | | |
| 24 HRS | 2.297 | 2.830 | 2.536 |
| 48 HRS | 3.619 | 6.722 | 3.599 |
| 72 HRS | 4.378 | 7.768 | 4.233 |
| 96 HRS | 4.741 | 7.617 | 4.377 |
| (3) MERIDIONAL WIND | | | |
| 24 HRS | 1.980 | 2.705 | 2.390 |
| 48 HRS | 2.361 | 3.093 | 3.168 |
| 72 HRS | 2.859 | 3.930 | 3.933 |
| 96 HRS | 3.569 | 4.743 | 3.584 |
| ABS.CORRELATION | | | |
| 24 HRS | 0.762 | 0.748 | 0.688 |
| 48 HRS | 0.563 | 0.473 | 0.476 |
| 72 HRS | 0.414 | 0.272 | 0.353 |
| 96 HRS | 0.180 | 0.158 | 0.337 |
| AND.CORRELATION | | | |
| 24 HRS | 0.883 | 0.854 | 0.857 |
| 48 HRS | 0.715 | 0.304 | 0.719 |
| 72 HRS | 0.550 | 0.142 | 0.573 |
| 96 HRS | 0.470 | 0.223 | 0.543 |

Table 3. RMSE, Absolute Correlation and Anomaly Correlation for Barotropic model, 1LPE model and Persistence. Initial state June 3, 1979.

Table 4. RMSE, Absolute Correlation and Anomaly Correlation for Barotropic model, 1LPE model and Persistence. Initial state June 4, 1979.

3.

JUNE 3, 1979

| | 1LPE | BARO | PERSIST |
|---|---|---|---|
| RMSE (M/SEC) | | | |
| (1) VECTOR WIND | | | |
| 24 HRS | 3.351 | 3.925 | 3.498 |
| 48 HRS | 4.470 | 4.924 | 5.446 |
| 72 HRS | 5.170 | 6.096 | 6.095 |
| 96 HRS | 5.740 | 6.540 | 5.937 |
| (2) ZONAL WIND | | | |
| 24 HRS | 2.589 | 3.154 | 2.411 |
| 48 HRS | 3.597 | 4.109 | 4.157 |
| 72 HRS | 4.167 | 5.191 | 4.734 |
| 96 HRS | 4.633 | 4.993 | 4.531 |
| (3) MERIDIONAL WIND | | | |
| 24 HRS | 2.128 | 2.337 | 2.535 |
| 48 HRS | 2.654 | 2.713 | 3.518 |
| 72 HRS | 3.059 | 3.196 | 3.839 |
| 96 HRS | 3.388 | 4.224 | 3.836 |
| ABS. CORRELATION | | | |
| 24 HRS | 0.712 | 0.698 | 0.697 |
| 48 HRS | 0.547 | 0.597 | 0.405 |
| 72 HRS | 0.349 | 0.349 | 0.257 |
| 96 HRS | 0.199 | 0.142 | 0.281 |
| AND. CORRELATION | | | |
| 24 HRS | 0.854 | 0.892 | 0.883 |
| 48 HRS | 0.660 | 0.604 | 0.621 |
| 72 HRS | 0.533 | 0.383 | 0.509 |
| 96 HRS | 0.519 | 0.520 | 0.575 |

4.

JUNE 4, 1979

| | 1LPE | BARO | PERSIST |
|---|---|---|---|
| RMSE (M/SEC) | | | |
| (1) VECTOR WIND | | | |
| 24 HRS | 3.734 | 3.908 | 3.873 |
| 48 HRS | 4.894 | 4.992 | 5.609 |
| 72 HRS | 5.961 | 5.667 | 5.963 |
| 96 HRS | 6.061 | 5.969 | 5.670 |
| (2) ZONAL WIND | | | |
| 24 HRS | 2.908 | 2.788 | 3.072 |
| 48 HRS | 3.880 | 3.644 | 4.229 |
| 72 HRS | 5.065 | 4.325 | 4.574 |
| 96 HRS | 4.929 | 4.535 | 4.606 |
| (3) MERIDIONAL WIND | | | |
| 24 HRS | 2.343 | 2.738 | 2.359 |
| 48 HRS | 2.983 | 3.412 | 3.684 |
| 72 HRS | 3.143 | 3.663 | 3.826 |
| 96 HRS | 3.528 | 3.881 | 3.306 |
| ABS. CORRELATION | | | |
| 24 HRS | 0.693 | 0.630 | 0.709 |
| 48 HRS | 0.463 | 0.420 | 0.389 |
| 72 HRS | 0.335 | 0.378 | 0.326 |
| 96 HRS | 0.186 | 0.340 | 0.388 |
| AND. CORRELATION | | | |
| 24 HRS | 0.802 | 0.842 | 0.799 |
| 48 HRS | 0.638 | 0.792 | 0.616 |
| 72 HRS | 0.558 | 0.723 | 0.582 |
| 96 HRS | 0.578 | 0.715 | 0.562 |

Table 5. Averaged RMSE

| Hours | Barotropic Model | | | | 1LPE Model | | | | | | |
|---|---|---|---|---|---|---|---|---|---|---|---|
| | | Yap('83) 1 | Yap('83) 2 | Adejokun (1983) | | Yap 1 | Yap 2 | Adejokun (1983) | Krish. (1980) | Ploshay (1977) | Persist. |
| **vector wind** | | | | | | | | | | | |
| 24 | 4.28 | 4.90 | 6.60 | 4.82 | 4.36 | 5.30 | 6.20 | 4.97 | 5.15 | 6.06 | 3.98 |
| 48 | 6.32 | 6.00 | 8.90 | 6.15 | 5.76 | 6.40 | 8.20 | 6.02 | 6.20 | 6.08 | 5.41 |
| 72 | 7.55 | 7.00 | 9.80 | 6.87 | 6.74 | 7.40 | 9.40 | 6.31 | - | 6.92 | 6.11 |
| 96 | 8.17 | 7.70 | 10.10 | 7.01 | 7.43 | 8.10 | 9.70 | 6.44 | - | 7.18 | 6.35 |
| **Zonal wind** | | | | | | | | | | | |
| 24 | 3.08 | 3.60 | 4.80 | 3.78 | 3.25 | 4.00 | 4.60 | 3.50 | - | - | 2.91 |
| 48 | 4.79 | 4.60 | 6.90 | 4.61 | 4.44 | 4.90 | 6.30 | 4.49 | - | - | 4.08 |
| 72 | 6.05 | 5.50 | 7.80 | 5.35 | 5.42 | 5.90 | 7.50 | 4.68 | - | - | 4.73 |
| 96 | 6.44 | 6.30 | 8.20 | 5.60 | 6.05 | 6.40 | 8.00 | 4.95 | - | - | 5.05 |
| **Meridional wind** | | | | | | | | | | | |
| 24 | 2.95 | 3.30 | 4.40 | 3.24 | 2.89 | 3.50 | 4.10 | 3.33 | - | - | 2.71 |
| 48 | 4.08 | 3.90 | 5.60 | 4.05 | 3.65 | 4.10 | 5.20 | 3.99 | - | - | 3.54 |
| 72 | 4.46 | 4.20 | 5.80 | 4.40 | 3.98 | 4.60 | 5.60 | 4.22 | - | - | 3.84 |
| 96 | 4.95 | 4.30 | 5.80 | 4.32 | 4.28 | 5.00 | 5.70 | 4.09 | - | - | 3.83 |

Table 6a. Domain Invariant for 1LPE Model.

| Hours | $\bar{Z}$ (m) | % Dept | $\bar{\zeta}_p$ ($m^{-1}s^{-1}$) | % Dept | $\bar{\zeta}_p^2$ ($m^{-2}s^{-2}$) | % Dept | $\bar{E}_T$ ($m^3s^{-2}$) | % Dept |
|---|---|---|---|---|---|---|---|---|
| | | | x $10^{-8}$ | | x $10^{-15}$ | | x $10^4$ | |
| 00 | 2064 | 0.00 | 0.5231 | 0.00 | 0.5458 | 0.00 | 2264 | 0.00 |
| 24 | 2074 | 0.47 | 0.5298 | 1.29 | 0.5343 | -2.10 | 2284 | 0.87 |
| 48 | 2073 | -0.05 | 0.5319 | 0.40 | 0.5276 | -1.25 | 2242 | -1.82 |
| 72 | 2035 | -1.84 | 0.5231 | -1.69 | 0.5243 | -0.63 | 2238 | -0.18 |
| 96 | 2070 | 1.71 | 0.5239 | 0.13 | 0.5221 | -0.41 | 2274 | 1.64 |
| Total | | 0.29 % | | 0.13 % | | -4.29 % | | 0.51 % |

Table 6b. Domain Invariant for Barotropic Model.

| Hours | $\bar{\zeta}_A$ ($s^{-1}$) | % Dept | $\bar{\zeta}_A^2$ ($s^{-2}$) | % Dept | $K_E$ ($m^2s^{-2}$) | % Dept |
|---|---|---|---|---|---|---|
| | x $10^{-4}$ | | x $10^{-9}$ | | x $10^2$ | |
| 00 | 0.1164 | 0.00 | 0.2507 | 0.00 | 0.2628 | 0.00 |
| 24 | 0.1156 | -0.63 | 0.2519 | 0.50 | 0.2859 | 8.76 |
| 48 | 0.1138 | -1.59 | 0.2524 | -0.38 | 0.3284 | 14.89 |
| 72 | 0.1121 | -1.52 | 0.2516 | -0.30 | 0.3372 | 2.67 |
| 96 | 0.1110 | -0.95 | 0.2512 | -0.14 | 0.3197 | -5.18 |
| Total Departure | | -4.69 % | | -0.32 % | | 21.14 % |

a

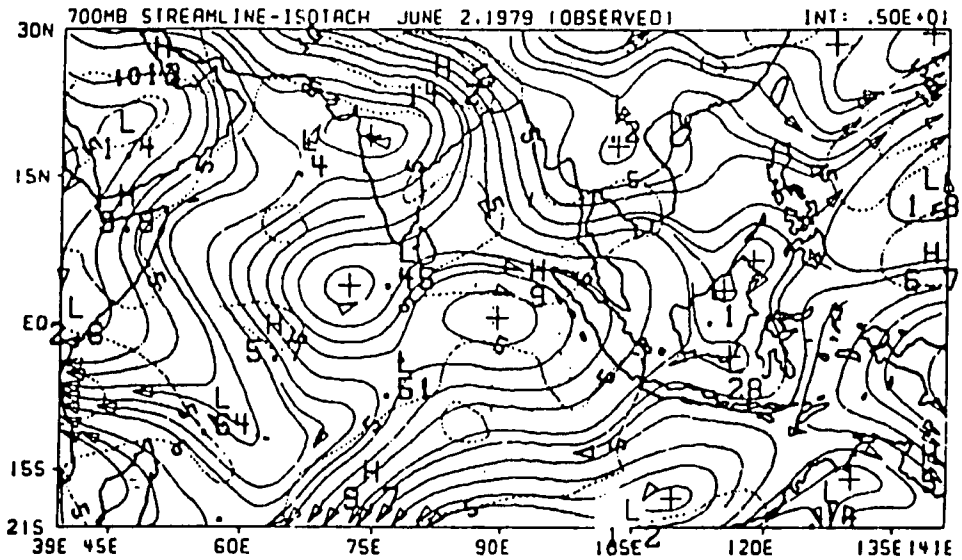


b.

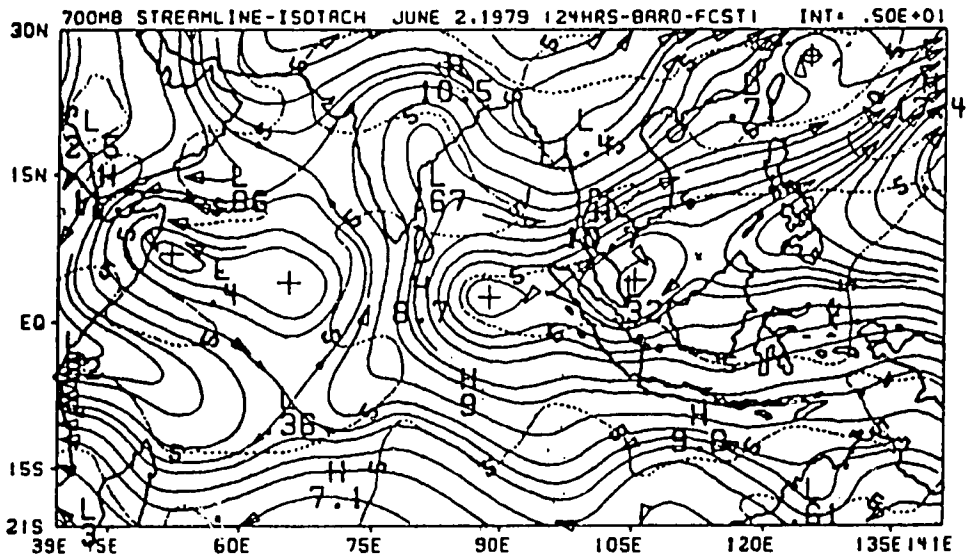


c.

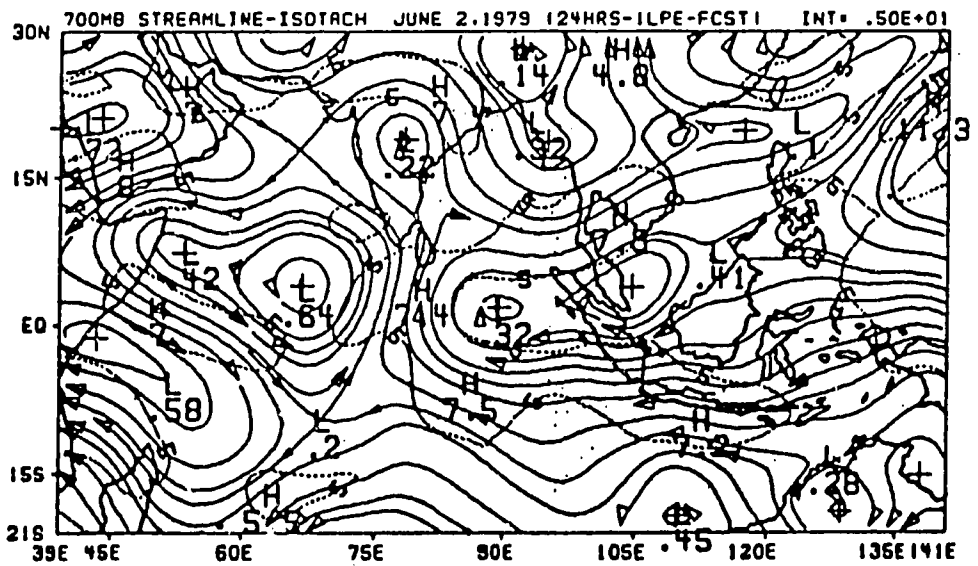


**Figure 1.** The 24 hours observed and predicted of 700 mb streamline (solid line) and isotachs (dotted line) in unit of m/sec. for initial state 12.00 GMT, June 2, 1979. a. Observed motion field. b. The 24 hours Barotropic forecast. c. The 24 hours ILPE forecast.

Figure 2. The 24 hours observed and predicted of 700 mb streamline (solid line) and isotachs (dotted line) in unit of m/sec. for initial state 12.00 GMT, June 3, 1979. a. Observed motion field. b. The 24 hours baro-tropic forecast. c. The 24 hours ILPE forecast.

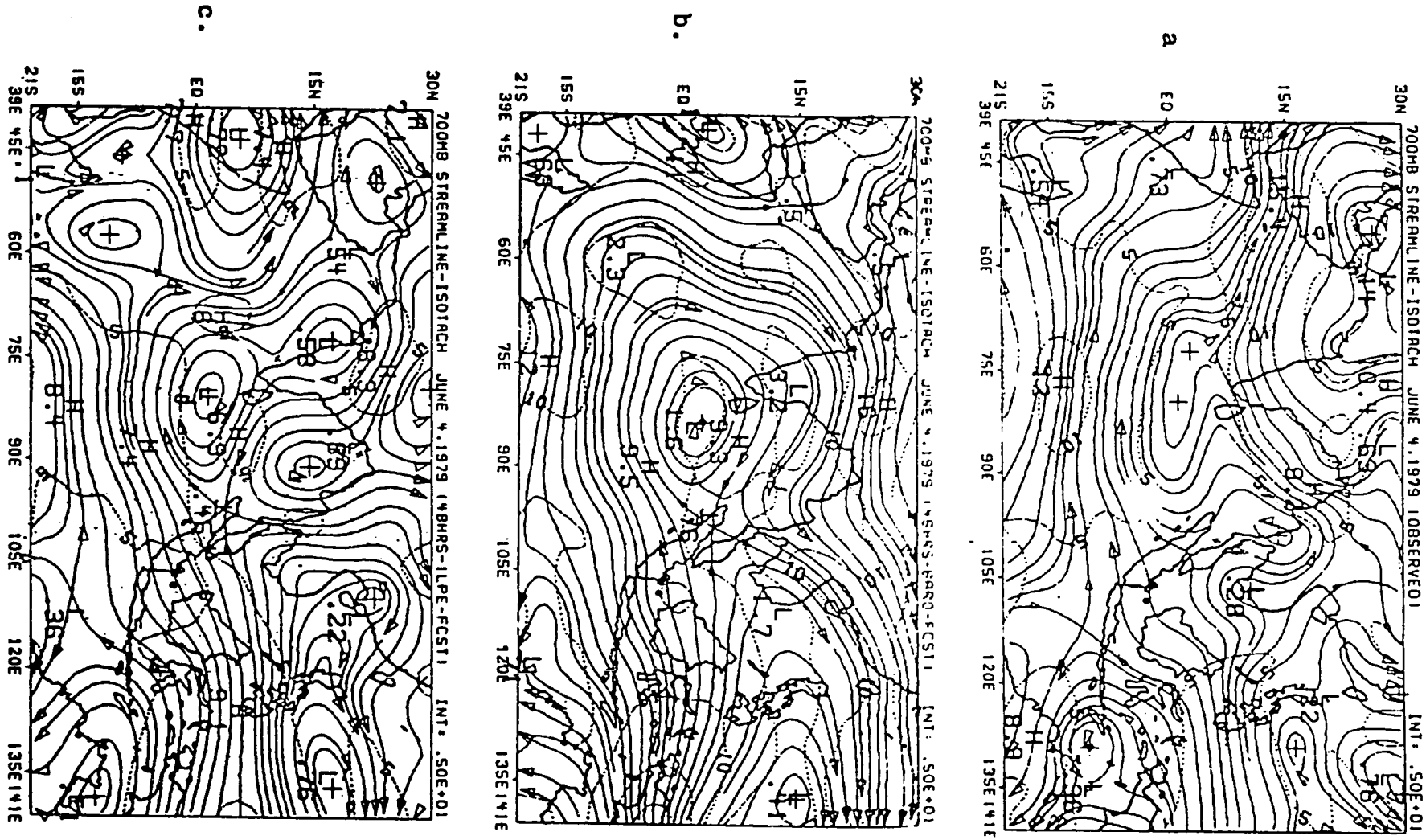


Figure 3. The 48 hours observed and predicted of 700 mb streamline (solid line) and isotachs (dotted line) in unit of m/sec for initial state 12.00 GMT, June 4, 1979. a. Observed motion field. b. The 48 hours Barotropic forecast. c. The 48 hours 1LPE forecast.

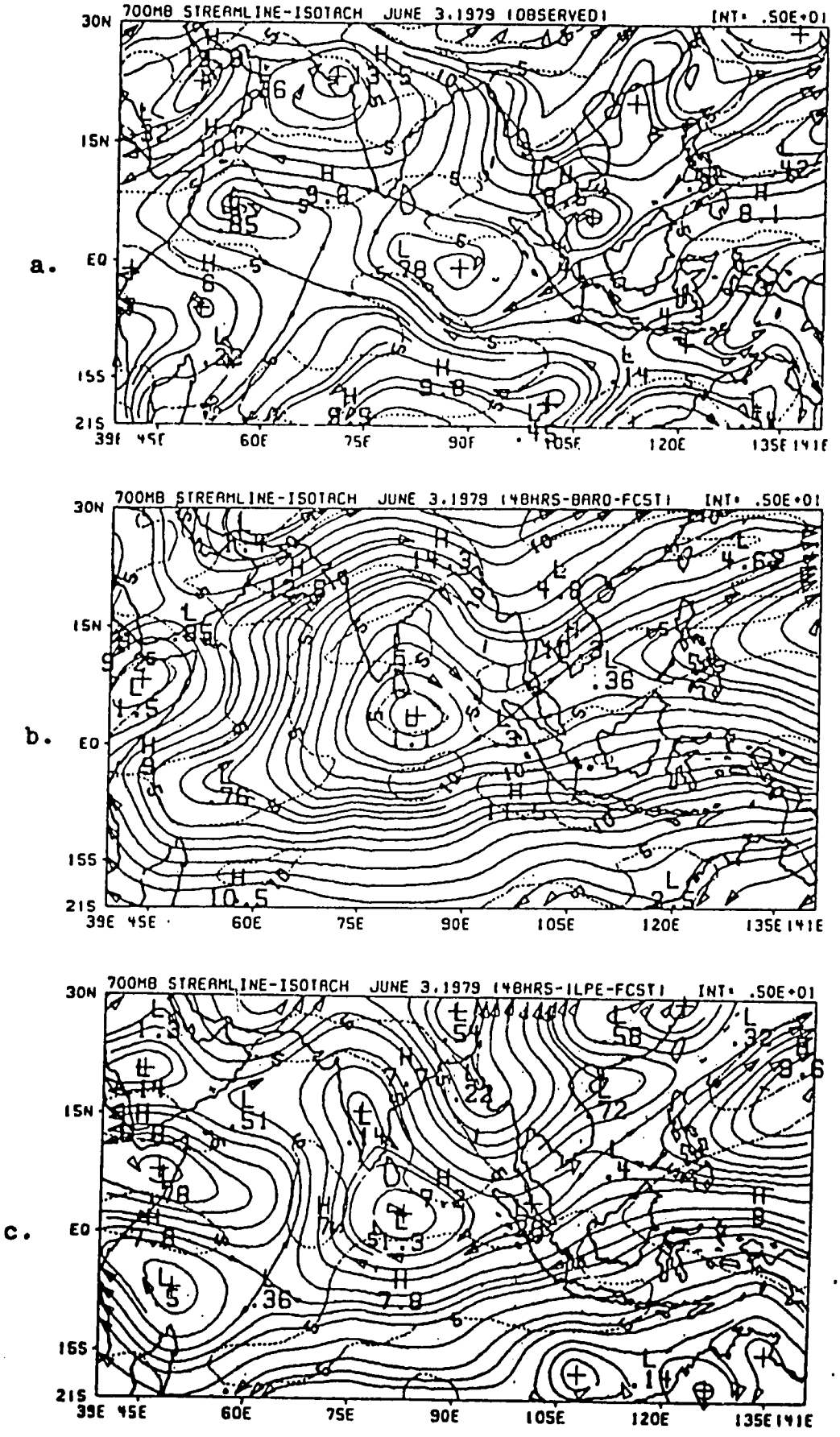


Figure 4. The 48 hours observed and predicted of 700 mb streamline (solid line) and isotachs (dotted line) in unit of m/sec. for initial state 12.00 GMT, June 3, 1979. a. Observed motion field. b. The 48 hours Barotropic forecast. c. The 48 hours 1LPE forecast.

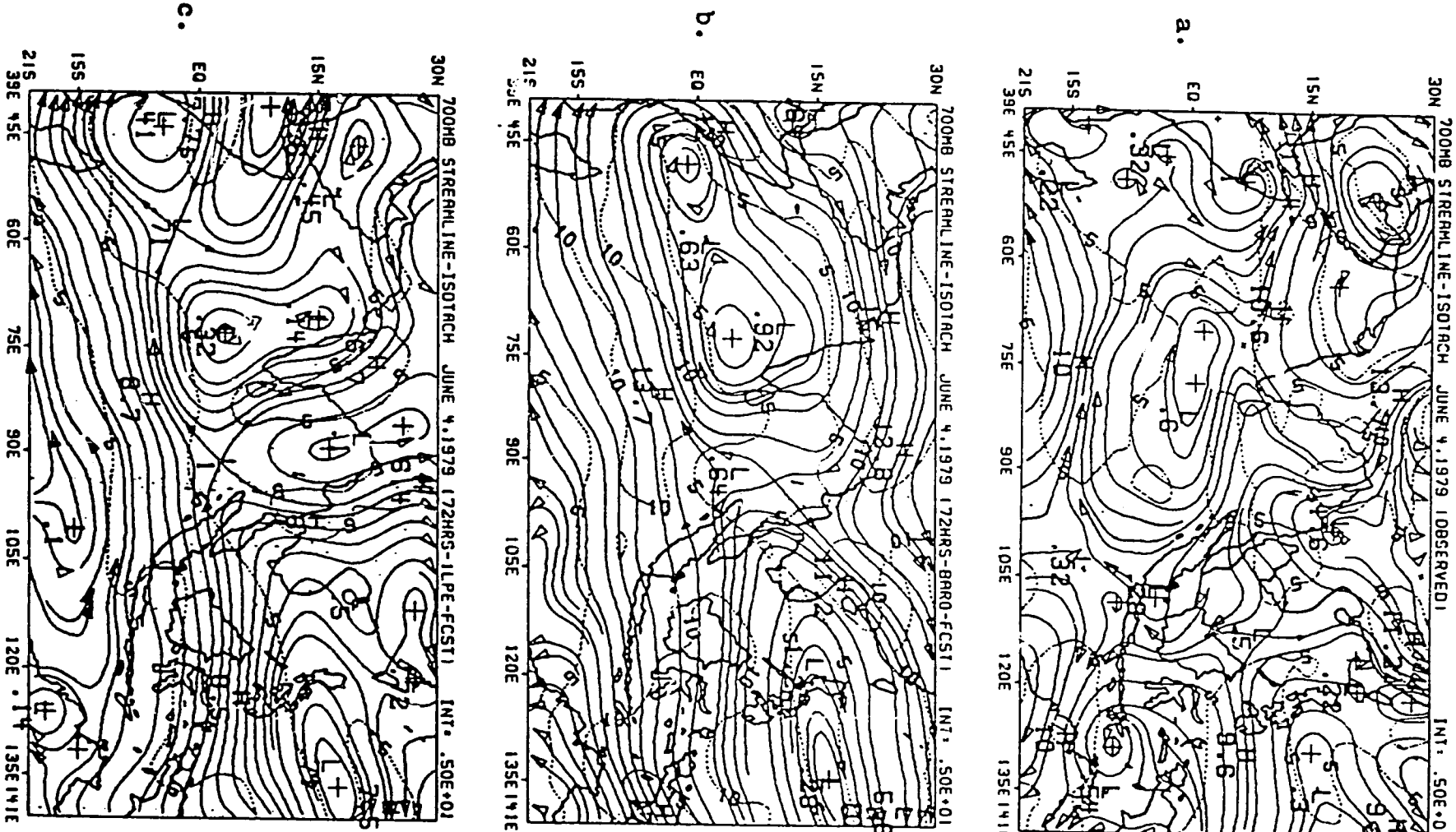


Figure 5. The 72 hours observed and predicted of 700 mb streamline (solid line) and isotachs (dotted line) in unit of m/sec. for initial state 12.00 GMT, June 4, 1979. a. Observed motion field. b. The 72 hours Barotropic forecast. c. The 72 hours ILPE forecast.

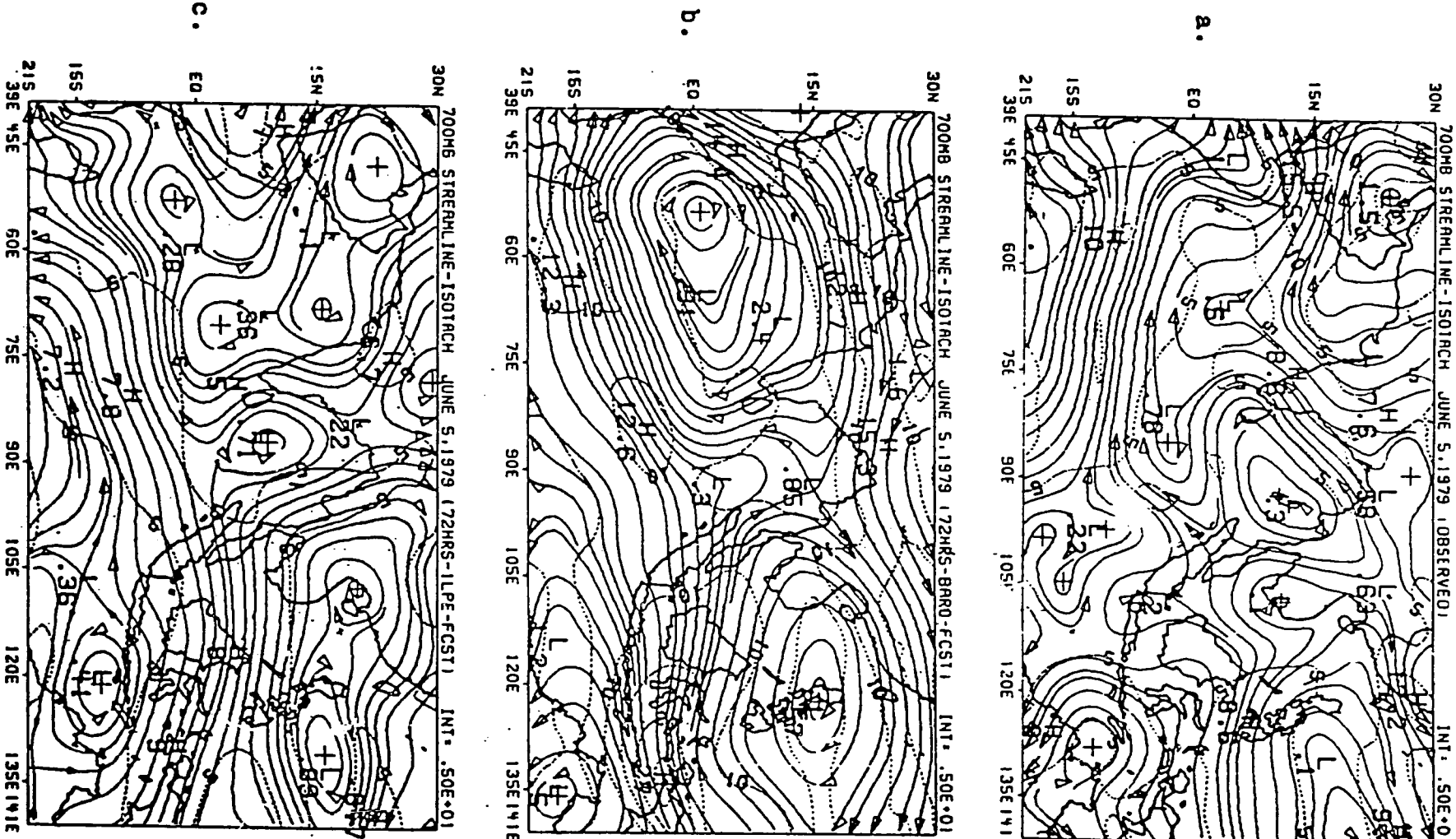


Figure 6. The 72 hours observed and predicted of 700 mb streamline (solid line) and isotachs (dotted line) in unit of m/sec. for initial state 12.00 GMT, June 5, 1979. a. Observed motion field. b. The 72 hours Barotropic forecast. c. The 72 hours 1LPE forecast.

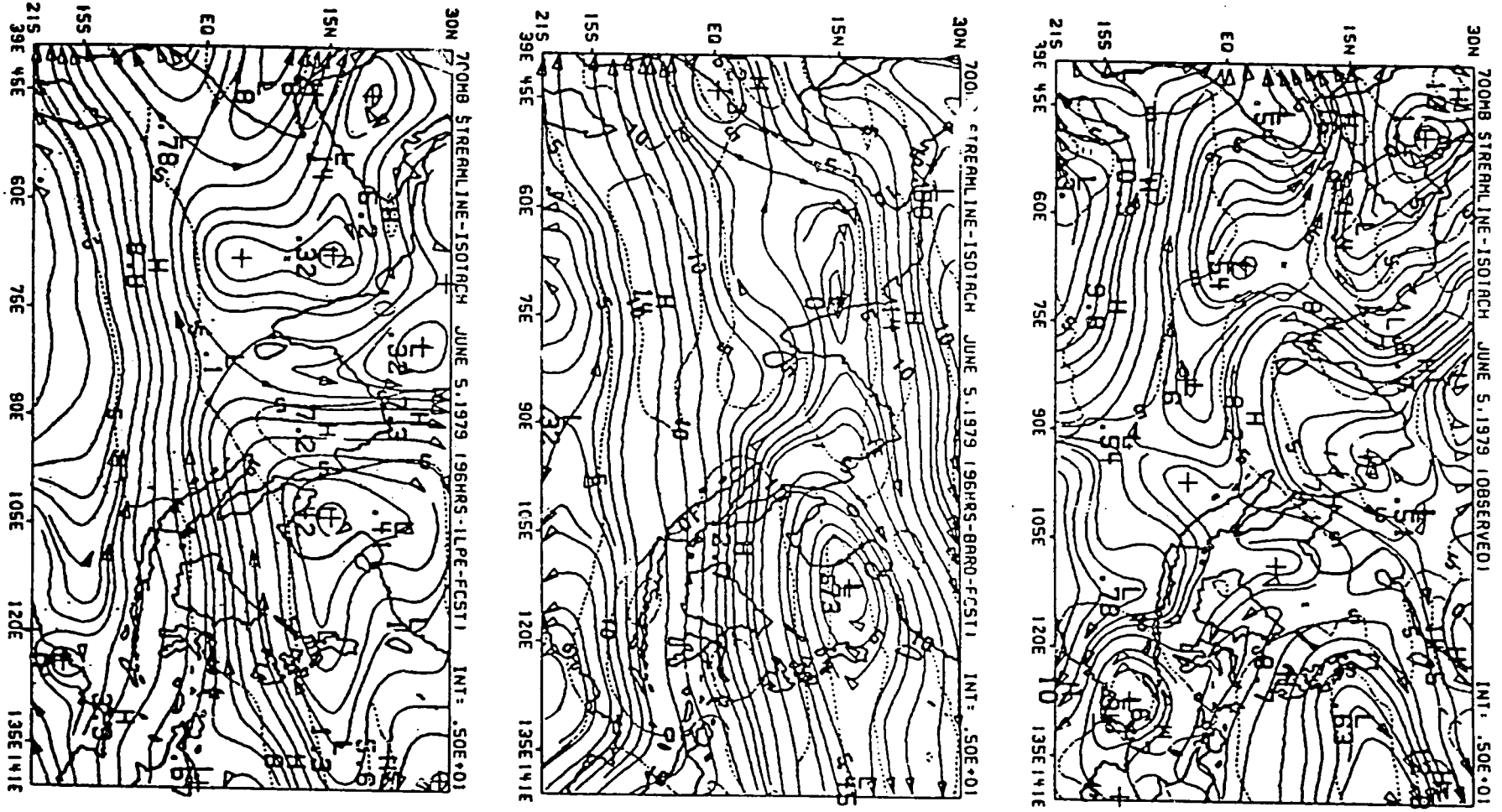


Figure 7. The 96 hours observed and predicted of 700 mb streamline (solid line) and isotachs (dotted line) in unit of m/sec. for initial state 12.00 GMT, June 5, 1979. a. Observed motion field. b. The 96 hours Barotropic forecast. c. The 96 hours 1LPE forecast.

# REFERENCES


Adejokun,J.A. and Krishnamurti,T.N.,1983, : Further numerical experiment on tropical waves, Tellus, 35A, 398-416.

Arakawa.A., 1966 : Computational design for longterm numerical integration of the equation of atmospheric motion, J. Comp. Phys. 1, 119-143.

Atkinson, G.D., 1971 : Forecasters' Guide to tropical meteorology, USAF Air Weather Service.

Findlater,J., 1969 : A major low level air current near Indian Ocean during the Northern summer, Quart.J.Roy.Met. Soc., 95, 362-380.

Gates, W.L. and Nelson, A.B., 1975 : A new (revised) tabulation of Scrips topography on 1° global grid. Part I : Terrain heights., Rept. No. R-1276-1-ARPA, Rand Corporation, Santa Monica, California.

Hollingsworth, A., Arpe,K., Tiedke, M., Capaldo, M., Savijarvi, H., Akesson, O. and Wood, J.A., 1979 : Comparison of Medium range Forecasts made with two parameterization schemes., ECMWF Tech. Rept. No. 13, ECMWF, Reading, England.

Kanamitsu, M. 1975 : On Numerical Prediction over a global tropical belt. Rept. No. 75-1, Dept. of Meteorology FSU, 282 pp.

Koteswaram, P., 1958 : The easterly jet stream in the tropic, Tellus, 10, 43-87.

Krishnamurti, T.N., 1971 : Tropical east-west circulation during northern summer., J. Atms. Sci., 28, 1342-1347.

_____, 1969 : An experiment in numerical prediction in equatorial latitude. Quart. J. Roy. Met. Soc., 95, 594-620.

_____, Ardanuy, P., Ramanathan, Y., Pasch, R.J., 1979 : Quick look summer Monex Atlas Part II the onset phase, Dept. of Meteorology FSU, Tallahasse, Florida.

Mathur, M.B., 1970 : A note on an improved quasi lagrangian advection scheme for primitive equations., Mon. Wea. Rev., 98, 214-219.

Matsuno, T., 1966 : Numerical integration of primitive equations by simulated backward difference method., J.Met.Soc. Japan, 44, 76-84.

Neimen, R., 1983 : Operational verification of ECMWF forecast field and results for 1980-1981 ECMWF. Tech. Rept. No. 36, 40 pp.

Ploshay, J.J., 1977 : Results of single level numerical prediction experiments during GATE., Master's thesis, FSU, Tallahassee, 88 pp.

Shuman, F.G., 1957 : Numerical methods in weather prediction II, Smoothing and filtering., Mon.Wea.Rev., 85, 357.

Yap, K.S., Tint, S., Krishnamurti, T.N., 1983 : Regional single level prediction experiments during winter monex., FSU Rept. No. , Tallahassee.